ACS Sustainable Chemistry & Engineering

Research Article

pubs.acs.org/journal/ascecg

A New Carbon/Ferrous Sulfide/Iron Composite Prepared by an in Situ Carbonization Reduction Method from Hemp (*Cannabis sativa* L.) Stems and Its Cr(VI) Removal Ability

Ru Yang,* Yong Wang, Min Li, and Yijie Hong

State Key Laboratory of Chemical Resource Engineering, Beijing Key Laboratory of Electrochemical Process and Technology for Materials, Beijing University of Chemical Technology, Beijing 100029, China

Supporting Information

ABSTRACT: A facile strategy is developed to prepare carbon/ferrous sulfide/iron (C/FeS/Fe) composites by an in situ carbonization reduction method using agricultural waste hemp stems as the carbon precursor and ferrisulfas as the iron source. Under the reductive atmosphere generated from biomass carbonization, ferrisulphas can be in situ directly decomposed and reduced into FeS/Fe at 800 °C existing in the form of nanoparticles embedded in a carbon matrix; so this synthetic procedure is much simpler compared with traditional multistep methods. The C/FeS/Fe composite, as expected, displays an excellent Cr(VI) removal performance with a maximum capacity of 127 mg/g at pH 5 because of the adsorption on its large surface and simultaneous reducing actions that have been evidenced by XPS analysis. Although the presence of FeS/Fe gives rise to an obvious decline of BET surface area, the strong reducibility can compensate for the loss of surface area and significantly enhance Cr(VI) removal especially at a low pH. The synergy between surface adsorption and FeS/Fe reduction under different pH makes this low-cost composite a potential material for treating contaminated water.

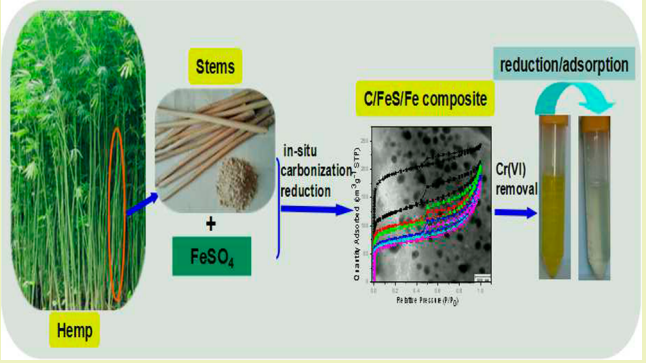

KEYWORDS: *Hemp, Carbon, Ferrous sulfide, Adsorption, Reduction, Hexavalent chromium*

INTRODUCTION

Porous carbon is a common adsorbent material in environmental protection, such as in water treatment, for its highly developed porosity, excellent adsorption capacity, and high degree of surface reactivity.[1] It can effectively adsorb contaminants in dependence with the van der Waals force, electrostatic attraction, or chemical bonds between surface functional groups and adsorbate.[2,3] However, the adsorption process primarily achieves phase transfer only and not transformation of some toxic pollutants into nontoxic or low toxic substances.[4] Hence, efforts must be made to synthesize functionalized and reactive porous carbons combining both adsorption and detoxification for environmental remediation.[4,5]

Hexavalent chromium (Cr(VI)), which is produced in a wide variety of industrial processes,[6] is such a poisonous contaminant, as specified by many agencies such as the United States Environmental Protection Agency (US EPA) and China's Ministry of Environmental Protection (MEP).[7,8] As one of the two stable forms of chromium in the natural environment, Cr(VI) is commonly present as soluble, mobile, and oxidizing oxyanions (CrO_4^{2-}, $HCrO_4^-$, and $Cr_2O_7^{2-}$) that have strong toxicity, causing carcinogenic and mutagenic effects and liver damage.[9−12] In contrast, trivalent chromium, (Cr(III)), usually found in the form of $Cr(OH)_3$ or Cr(III) complexes with organic ligands, is less soluble, less mobile, and thereby less toxic.[13,14] It is even considered a nontoxic and essential trace metal in human nutrition (especially in glucose metabolism).[15,16] Thus, it is of great importance to transform Cr(VI) to Cr(III) and fundamentally reduce the toxicity when porous carbons are used to adsorb Cr(VI) from contaminated water.[17]

Actually, porous carbon itself can reduce a small part of Cr(VI) to Cr(III) by redox reactions of surface functional groups, yet this effect is relatively weak.[18,19] To promote the reduction, some reducing agents such as zero valent iron, ferrous iron, and iron sulfide[20−22] can be introduced onto porous carbon. Recently, several elegant works about activated carbon/nanoscale zero valent iron composite, iron-doped ordered mesoporous carbon, and nanosized magnetite-coated activated carbon have been reported,[23−25] while limited researches have been carried out to integrate ferrous sulfide with porous carbon. Ferrous sulfide, a nontoxic and low-cost natural mineral, is an effective reductant for a toxic oxidized species.[26−28] Due to the high reducibility provided by both

Received: February 14, 2014
Revised: March 16, 2014
Published: April 8, 2014

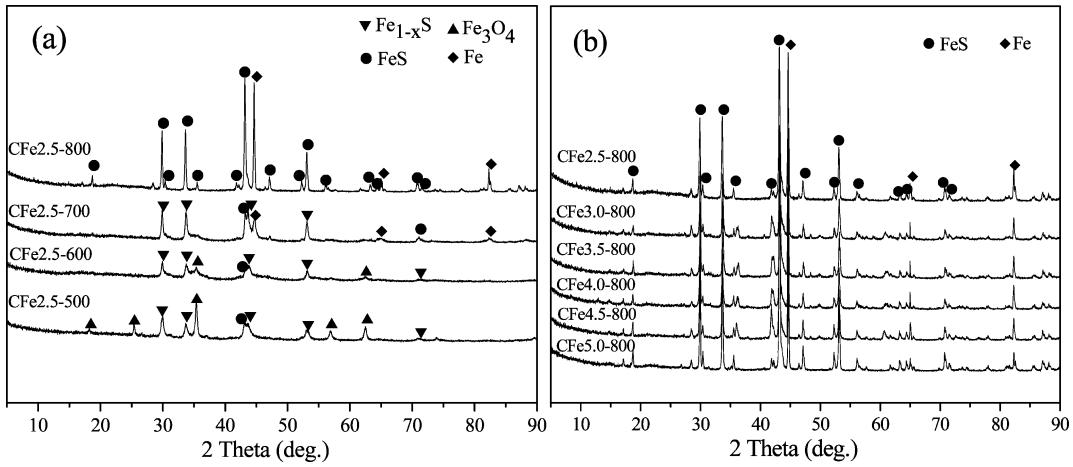

Figure 1. XRD patterns of as-prepared samples (a) with 2.5 mmol of $FeSO_4$ at different temperatures and (b) with various $FeSO_4$ dosages at 800 °C.

Fe(II) and S(−II), it is far more efficient to reduce Cr(VI) than iron-bearing oxide minerals, and the generated products during redox reactions could greatly decrease the chance of chromium reoxidation.[21] A type of carbon/pyrite composite exhibiting a potential environmental remediation application in the removal of trichloroethylene has been successfully synthesized via sequential processes, including incipient wetness iron impregnation, transformation into iron oxides by calcination, and sulfurization under further heat treatment, in addition to the previous preparation of bituminous-coal-based carbon.[4] However, the multi-step synthesis and high-cost raw materials still propel us to explore more facile and more economical preparation routes.

Currently, biomass is undoubtedly the cost-optimal raw material for producing porous carbons, particularly the lignocellulosic biowaste, such as sawdust, husk, stalk, and paper sludge.[29−34] Some biomass-derived carbons have been endowed with superior performance through doping and modification. For instance, corncob carbon coated with magnetite- and Fe-modified activated carbon from *Trapa natans* husk showed good Cr(VI) removal ability from aqueous solutions.[24,35] Hemp is a widely planted annual herbaceous crop around the world, and in China alone, its planting area will increase to about 670,000 hectares in 2020.[36] Hempseed is an important feedstock for oil, and hemp bast provides fibers for the textile industry. Hemp bast fiber has also been used as a precursor for high performance carbon, which could play an active role in water purification and supercapacitors.[37−39] Yet as a byproduct, hemp stem is of little use and deserves further development. Although hemp stems have been reported to prepare activated carbons for the adsorption of water vapor and hydrogen,[36,40] producing novel materials with new performances from hemp stems will still make perfect sense. Like other biowaste, the carbonization of hemp stems can generate a reducing atmosphere, which is obviously worth exploiting during material preparation.

Herein, we introduce an in situ carbonization reduction method to prepare a new C/FeS/Fe composite by the copyrolysis of hemp stems and ferrisulfas in flowing N_2. Ferrisulfas can be directly decomposed and reduced into FeS/Fe nanoparticles embedded in carbon under the reducing atmosphere generated from hemp stem carbonization, and meanwhile, it acts as an activating agent to develop pores in carbon matrix. The in situ synthetic process saves time, and more importantly, the obtained porous C/FeS/Fe composite displays good simultaneous adsorption and reduction performance on Cr(VI) removal, which makes it a potential material in the fields of chemical industry and environmental protection. The study is significant for the hemp-growing regions, especially for those under pressure of chromium pollution, such as China's Yunnan province. Furthermore, producing functionalized carbon composites from agricultural wastes for wastewater treatment should be a promising sustainable way to realize waste control by using waste.

EXPERIMENTAL SECTION

Materials Preparation. Hemp stems, taken from "Yunma 1" after the hemp harvest in Menghai County, Xishuangbanna Dai Autonomous Prefecture, Yunnan Province of China, were smashed into powder (400 meshes). One gram of hemp stem powder and 2.5 mmol of $FeSO_4·7H_2O$ were mixed in 40 mL of deionized water, stirred for 3 h, and dried in an oven. The $FeSO_4$-impregnated hemp stems were carbonized to 800 °C at a heating rate of 5 °C/min and then maintained at 800 °C for 2 h in a tube furnace. Other composites were similarly produced at different temperatures (500−700 °C) and with various amounts of $FeSO_4·7H_2O$ (3.0−5.0 mmol). The obtained samples were referred to as CFe*a*-*b*, where *a* and *b* respectively represented the number of millimoles of $FeSO_4·7H_2O$ and the carbonization temperature. The total mass fraction of iron compounds on carbon was obtained by adding 0.1 g of product into 50 mL of 0.5 M HCl solution and calculating the mass difference. As a comparison, the blank carbon named C-800 was also prepared by directly carbonizing hemp stems at 800 °C. All chemicals used in the experiment were analytical reagent grade.

Characterization. XRD patterns were recorded on a Rigaku D/max2500B2+/PCX system operating at 40 kV and 20 mA using Cu Kα radiation (λ = 1.5406 Å). Fourier transform infrared spectra (FTIR) were acquired using a Nicolet 8700 FTIR spectrometer by averaging 256 scans in the 4000−400 cm^{-1} spectral rang at 4 cm^{-1} resolution. Nitrogen adsorption−desorption isotherms were measured at −196 °C with a Micromeritics ASAP2020 instrument. HRTEM measurement was conducted on JEM 2010 electron microscopes. XPS analysis was performed using an ESCALAB250 (Thermo VG, U.S.A.). The leakage of iron and total chromium in solution were determined with an ICP-MS7700 (Agilent) instrument.

Cr(VI) Removal Experiments. The stock solution of Cr(VI) was prepared at a concentration of 100 mg/L from water-soluble metallic salt ($K_2Cr_2O_7$). The other water samples were the diluted solution from the stock one with deionized water. For pH adjustment, 0.1 M NaOH and 0.1 M HCl were prepared.

Batch equilibrium studies were performed by mixing 0.1 g of sorbent with 100 mL of $K_2Cr_2O_7$ solution in conical flasks shaken at a

certain frequency to reach equilibrium at room temperature. Then, the mixture was filtered, and the residual Cr(VI) concentration was measured according to the diphenylcarbazide method[41] with a UV−vis spectrophotometer (UV-752, Shanghai) at a wavelength of 540 nm. Using a similar approach, the effect of initial pH on Cr(VI) removal was investigated in the contact time.

The Cr(VI) removal amount q_t (mg/g) and removal efficiency at any time t (min) can be calculated from

$$q_t = (C_i - C_t)V/W \quad (1)$$

$$\text{Removal } \% = 100(C_i - C_t)/C_i \quad (2)$$

where C_i and C_t (mg/L) are, respectively, the concentrations of Cr(VI) at initial time and time t, V (L) is the volume of the solution, and W (g) represents the amount of sorbent. The equilibrium removal amount and equilibrium concentration are written as q_e (mg/g) and C_e (mg/L), respectively.

RESULTS AND DISCUSSION

Characterization of As-Prepared Samples. The phase composition of as-prepared samples are characterized by XRD patterns shown in Figure 1. It is found that the major components on carbon vary with temperatures from 500 to 800 °C (Figure 1a). At 500 °C, Fe_3O_4, $Fe_{1-x}S$, and FeS are generated from the decomposition of $FeSO_4$ under a reductive atmosphere provided by the carbonization of biomass (eqs 1−4, Supporting Information).[42,43] The peaks of Fe_3O_4 decrease at 600 °C and disappear at 700 °C, and simultaneously, simple substance iron is detected as a result of the reduction of Fe_3O_4 by CO or carbon, while $Fe_{1-x}S$ and FeS phases increase gradually with the temperature increasing to 700 °C (eqs 4−7, Supporting Information). There are only FeS and Fe detected after the carbonization at 800 °C because of the complete transformation of $Fe_{1-x}S$ and Fe_3O_4 (eqs 5−8, Supporting Information), which is in correspondence with the research finding about $FeSO_4$ decomposition in a reductive atmosphere.[42] According to eq 7 of the Supporting Information, elemental sulfur is also generated, but no peak hints at the existence of a sulfur crystal, indicating that sulfur may be amorphous or microcrystalline that cannot be detected by XRD.[44] When $FeSO_4$ dosages increase from 2.5 to 5.0 mmol, FeS and Fe are identical products for all the samples regardless of the $FeSO_4$ dosage (Figure 1b), suggesting that $FeSO_4$ should be completely transformed into FeS and Fe during the carbonization of hemp stems. The variation of $FeSO_4$ dosage finally affects the mass fraction of FeS/Fe loaded on carbon (Table S1, Supporting Information). Therefore, the in situ carbonization reduction method will lead to successful preparation of a C/FeS/Fe composite at 800 °C.

FTIR spectra in Figure 2 help to identify the variation of surface functional groups of as-prepared samples. The bands at 3450, 1620, 1560, and 1060 cm^{-1} are, respectively, assigned to the stretching of O−H, C═O, aromatic C═C, and C−O groups,[45,46] and the intensity of O−H, C═O, and C−O decreases with rising temperature because of dehydrogenation and deoxygenation. The bands at 876 and 592 cm^{-1} correspond to S═O deformation vibrations, implying that $FeSO_4$ has a sulfurization effect on carbon.[47,48] The spectrum of the C/FeS/Fe composite exhibits three small peaks at 425, 619, and 1120 cm^{-1}, which may be attributed to Fe−S bonds. All the results indicate that the prepared samples are abundant in oxygen- and sulfur-containing groups, which have been considered favorable for the removal of chromium from water.[49,50]

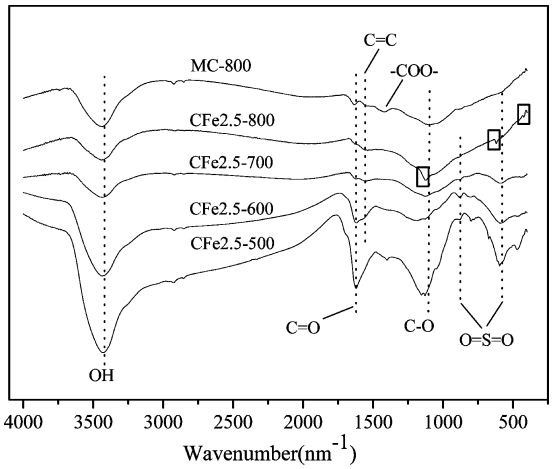

Figure 2. FTIR spectra of blank carbon and prepared composites with 2.5 mmol of $FeSO_4$ at different temperatures.

Figure 3 gives HRTEM images of the C/FeS/Fe composite. It is shown that sphere-like nanoparticles in diameter of 50−100 nm are homogeneously dispersed in carbon matrix.

The selected area EDAX inserted in Figure 3a demonstrates that the particles are composed of iron and sulfur. On the basis of XRD analysis, the crystal lattice fringes in Figure 3b with the spacing values of 1.433 and 1.202 Å are, respectively, consistent with those of the (200) and (307) diffraction peaks of Fe and FeS. The symbiosis of these two substances can also be intuitively observed. Despite the aggregation, Fe mainly exists on the periphery of the particle, in close proximity to carbon, suggesting its origin from carbon reduction of iron compounds.

The porous structures of the as-prepared samples are studied by N_2 adsorption−desorption technique. It is shown in Figure 4 that all the adsorption isotherms belong to a mixed type in the IUPAC classification, whose initial part is type I with an important uptake at low relative pressures and the remaining part is type IV with a type H4 hysteresis loop associated with slit-like pores.[51] The steep rise of the initial part signifies a large proportion of micropores, and the obvious hysteresis and the cocked "tail" at high relative pressure indicate the presence of mesopores and macropores. In Figure 4a, as temperature rises, the quantity adsorbed at low relative pressure increases, the hysteresis loop enlarges, and the "tail" becomes prominent, indicating an increase in various pores. The C/FeS/Fe composite obtained at 800 °C displays the highest nitrogen uptake, which is attributed to the most abundant pores generated from the enhanced metal-catalyzed gasification reactions of carbon at high temperature.[52] In Figure 4b, the N_2 uptake continuously decreases with an increase in $FeSO_4$ dosage because of the decline of micropores despite the increase in meso/macropores, suggesting that more $FeSO_4$ would help to develop more meso/macropores at the expense of destroying micropores. The pore size distributions of the as-prepared samples show multi-modal distributions with a distinct maxima in micropores and broad meso/macropore regions (Figure S1, Supporting Information). From the textural parameters calculated from N_2 adsorption isotherms (Table 1), it is shown that the BET surface area, total pore volume, micropore volume, and average pore diameter all increase with carbonization temperature, and the average pore diameter keeps increasing with an increase in $FeSO_4$ dosage, while the BET specific surface area and micropore volume decrease.

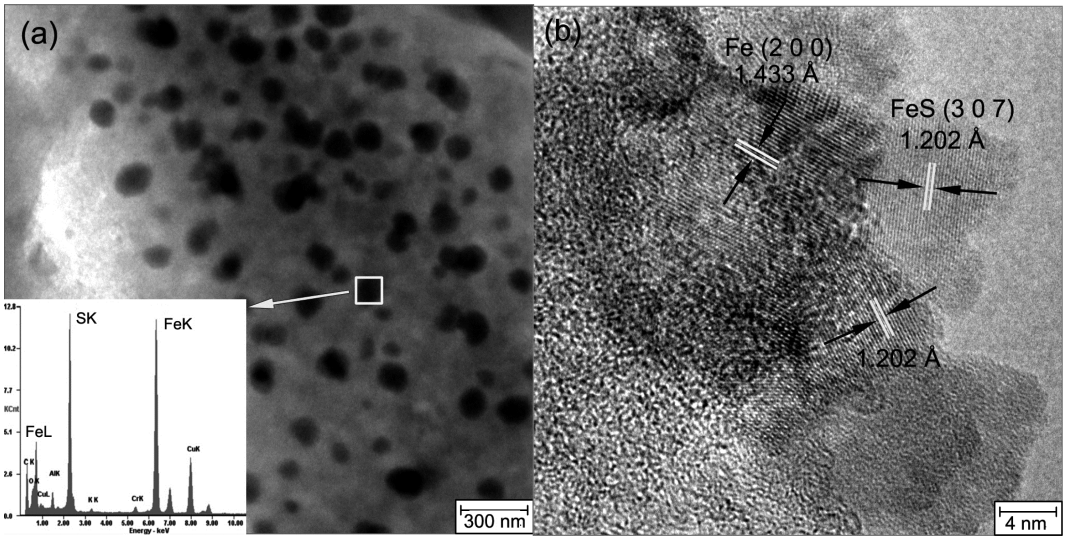

Figure 3. HRTEM images of (a) C/FeS/Fe composite (inset: EDAX spectrum) and (b) crystal lattice fringes.

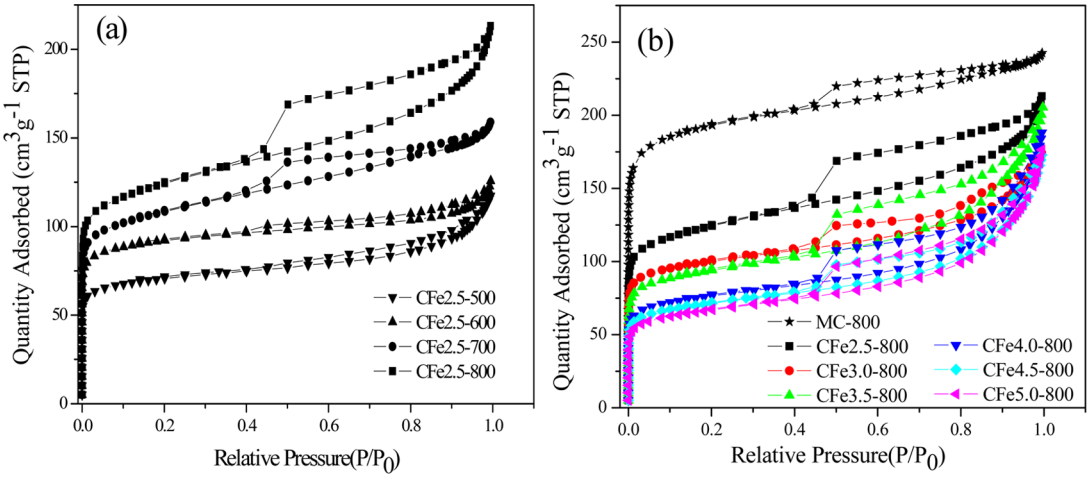

Figure 4. N_2 adsorption−desorption isotherms of as-prepared samples (a) with 2.5 mmol of $FeSO_4$ at different temperatures and (b) with various $FeSO_4$ dosages at 800 °C.

Table 1. Textural Parameters Deduced from N_2 Adsorption at −196 °C on As-Prepared Samples

						DFT method	
sample	carbonization temperature (°C)	$FeSO_4·7H_2O$ amount (mmol)	S_{BET} (m^2 g^{-1})	V_{total} (cm^3 g^{-1})	D_{ave} (nm)	V_{micro} (cm^3 g^{-1})	V_{meso} (cm^3 g^{-1})
C-800	800	0	598	0.375	2.51	0.237	0.0649
CFe2.5-500	500	2.50	220	0.181	2.69	0.0596	0.0316
CFe2.5-600	600	2.50	285	0.193	2.71	0.117	0.0210
CFe2.5-700	700	2.50	344	0.246	2.86	0.126	0.0637
CFe2.5-800	800	2.50	395	0.330	3.34	0.140	0.0933
CFe3.0-800	800	3.00	314	0.320	3.44	0.111	0.0771
CFe3.5-800	800	3.50	298	0.318	4.27	0.107	0.150
CFe4.0-800	800	4.00	242	0.291	4.81	0.0671	0.0929
CFe4.5-800	800	4.50	227	0.267	4.71	0.0760	0.0965
CFe5.0-800	800	5.00	214	0.273	5.10	0.0499	0.0992

Sample CFe2.5-800 has the largest BET surface area of 395 m^2/g among the obtained composites, which is still smaller than that of the blank sample C-800. The results indicate that an increase in temperature is conducive to developing porous structures, and introducing $FeSO_4$ can help to enlarge pores but will give rise to a reduction in specific surface area.

Cr(VI) Removal Properties. The Cr(VI) removal capacity−BET specific surface area relationship for samples at different temperatures (Figure 5a) shows that the Fe-containing sample prepared at high temperature has a higher Cr(VI) removal capacity than the one obtained at lower temperature because, on the one hand, the specific surface area increases with temperature, and, on the other hand, high temperature

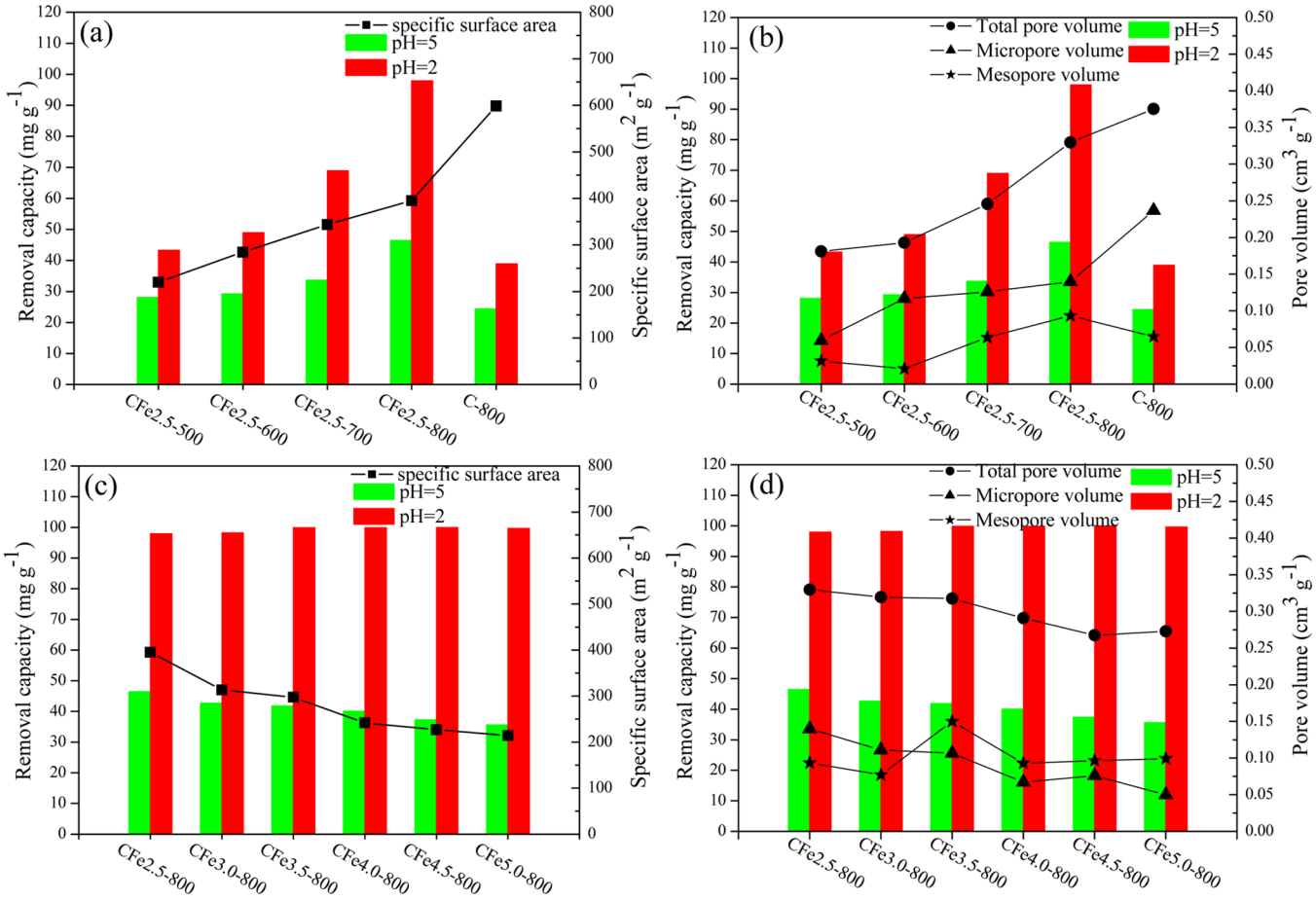

Figure 5. Variation of Cr(VI) removal capacity with textural parameters of as-prepared samples at pH 5 and 2 (Concentration, 100 mg/L; carbon dosage, 1.0 g/L).

carbonization results in low carbon yield and a relatively high content of iron compounds (Table S1, Supporting Information). The blank sample C-800 with the largest surface area of all presents the lowest Cr(VI) removal capacity, suggesting that iron compounds introduced on carbon should be very favorable to enhance the removal of Cr(VI). As expected, the C/FeS/Fe composite CFe2.5-800 displays the best performance, with about 100% of Cr(VI) being removed at pH 2. The removal capacity at pH 2 for each sample is higher than that at pH 5, indicating that a lower pH may benefit Cr(VI) removal. The Cr(VI) removal capacity−pore volume relationship for samples at different temperatures (Figure 5b) shows that the removal capacity of samples aside from C-800 increase with an increase in total pore volume, micropore volume, and mesopore volume, which is analogous to the changing trend with surface area. These results make us believe that the porous structure plays an important role in the removal of Cr(VI) despite the presence of iron compounds. When $FeSO_4$ dosage is changed (Figure 5c and d), the Cr(VI) removal capacity is positively related to the BET surface area and pore volumes and negatively correlated to $FeSO_4$ dosage at pH 5, while at pH 2, there is no obvious correlation with pore structure parameters as nearly 100% of Cr(VI) can be removed by all the C/FeS/Fe composites. This implies that FeS/Fe should make a dominating contribution at pH 2 because of its strong reducibility; however, the effect of surface adsorption overwhelms that of reduction at a higher pH, which becomes the predominant factor. According to the experimental results, it can be determined that the C/FeS/Fe composite CFe2.5-800 has an excellent Cr(VI) removal performance whether at pH 5 or 2, owing to the combination of adsorption on its large surface area and reduction by FeS/Fe.

The surface chemistry of CFe2.5-800 prior to and after Cr(VI) removal at pH 5 and 2 has been characterized by XPS to investigate the removal mechanism by C/FeS/Fe composite. The wide survey scan shows the detected elements in Figure 6a. The decrease of the C 1s signal and the enhancement of O 1s intensity demonstrate the obvious change of their relative content after treatment at pH 5 and 2, suggesting that chemical reactions have occurred during Cr(VI) removal. The C 1s spectra in Figure 6b are deconvoluted into four peaks at 284.8, 286, 286.8, and 289.3 eV, which are, respectively, assigned to aromatic or aliphatic carbon (C−C, C−H), phenolic and alcohol carbon (−C-O), carbon present in carbonyl or quinone groups (C═O), and carboxyl or ester groups (O−C═O).[45,53] Although the relative content of carbon decreases with decreasing pH (Table S2, Supporting Information), the percentage of C═O groups, as a portion of surface carbon atoms, increases after Cr(VI) removal because of the generation of new C═O groups from the original carbon functional groups (eqs 9 and 10, Supporting Information).[54,55] For the O 1s spectra in Figure 6c, two peaks at 530.8 and 532.4 eV are, respectively, assigned to carbonyl oxygen of quinines and carbonyl oxygen atoms in esters and anhydrides or oxygen atoms in hydroxyl groups; one peak at 533.7 eV is associated with noncarbonyl oxygen atoms in esters and anhydrides.[56] Apparently, C═O groups also increase after Cr(VI) removal,

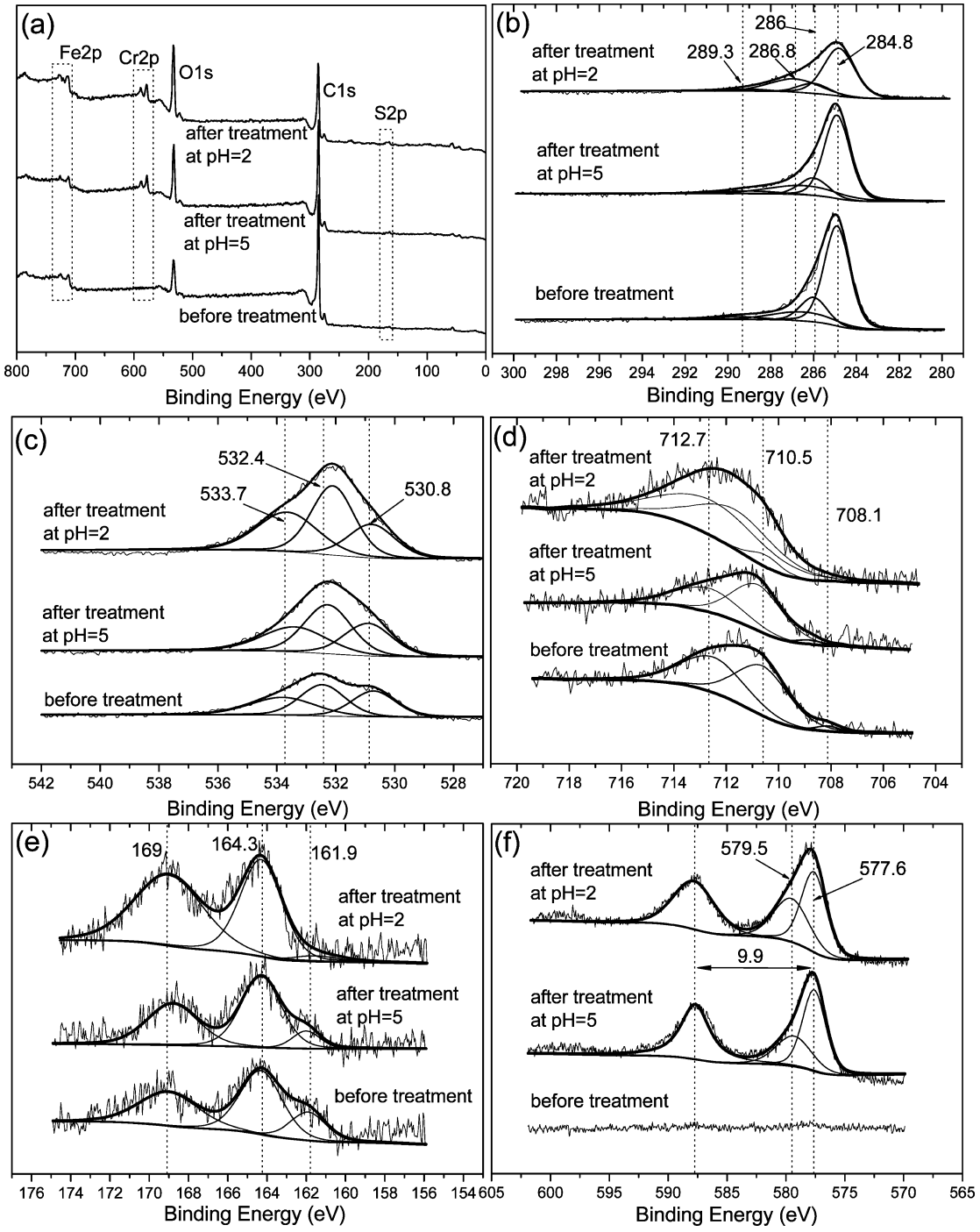

Figure 6. XPS spectra of C/FeS/Fe composite prior to and after Cr(VI) removal at pH 5 and pH 2: (a) wide survey scan, (b) C 1s, (c) O 1s, (d) Fe 2p3/2, (e) S 2p, and (f) Cr 2p spectra.

which is in accordance with the results obtained from the C 1s spectra. The consumption of protons (eqs 9 and 10, Supporting Information) indicates that a lower pH will facilitate the reduction of $HCrO_4^-$ by the carbon surface.

The Fe 2p3/2 spectra presented in Figure 6d involve three contributions. The first peak located at 708.1 eV corresponds to Fe(0). The second at 710.5 eV is attributed to Fe(II), and the third is attributed to Fe(III) lying between 711.6 and 712.7 eV.[57−60] Before Cr(VI) removal, only a little Fe(0) can be detected because most of the Fe(0) on the particle surface may be oxidized, and the surface sensitivity of XPS can only detect the photoelectrons from the top few tens of angstroms.[61] After Cr(VI) removal at pH 5, the Fe(0) and Fe(II) peaks move to higher binding energies, indicating the transformation to high valence iron. At pH 2, only Fe(III) can be detected as a result of Cr(VI) oxidization (eqs 11−13, Supporting Information). There is an increasing percentage of iron after treatment at pH 2 probably because of the attachment of dissolved iron ions on the carbon surface through adsorption and complexation.[46] XRD analysis has also been used to investigate the phase composition in the core of FeS/Fe particles after Cr(VI) removal (Figure S2, Supporting Information). It can be seen that zero valent iron still exsits after Cr(VI) removal at pH 5,

dx.doi.org/10.1021/sc500092z | ACS Sustainable Chem. Eng. 2014, 2, 1270−1279

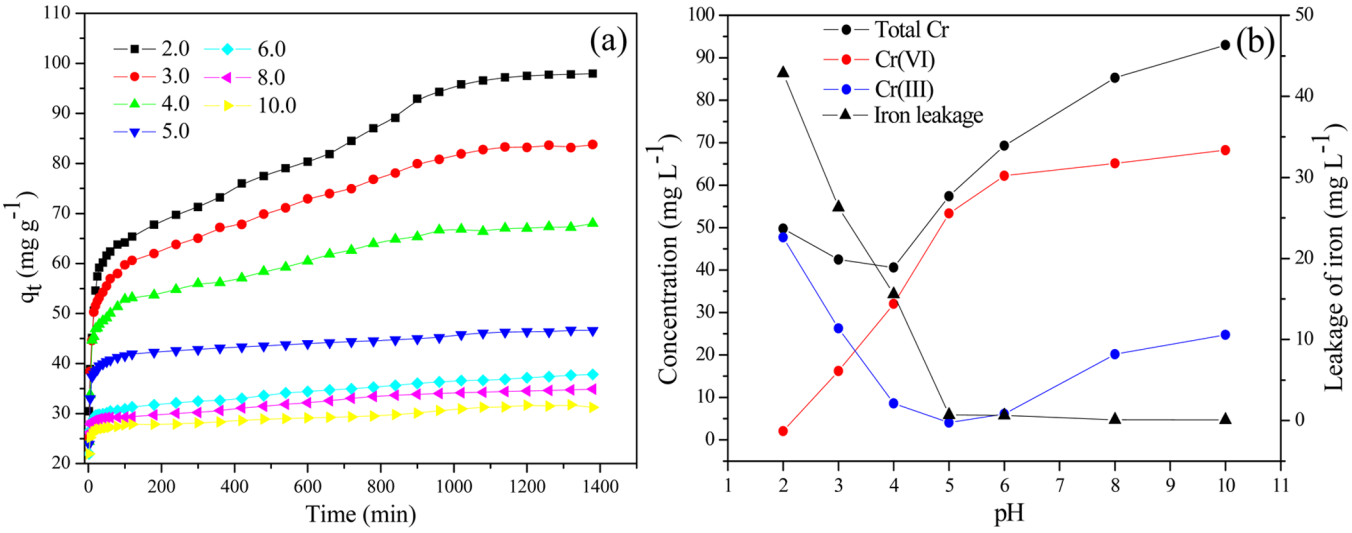

Figure 7. (a) Effect of contact time and initial pH on the removal of Cr(VI) by a C/FeS/Fe composite and (b) effect of initial pH on Cr species concentration and iron leakage. (Initial concentration, 100 mg/L; carbon dosage, 1.0 g/L).

although it has not been detected by XPS. However, disappears at pH 2 because of the strong acidic solution.

The S 2p spectra in Figure 6e exhibit three species: S(−II) at 161.9 eV,[22] elemental S(0) at 164.3 eV,[60] and SO_4^{2-}/−SO_3H at 169 eV.[62,63] Elemental S(0), which is not detected by XRD, can be observed by XPS. The intensity of the S(−II) signal decreases, and the S(0) and SO_4^{2-}/−SO_3H signals dramatically increase after Cr(VI) removal, suggesting that S(−II) can be oxidized into S(0) and SO_4^{2-} by Cr(VI) in an acid environment (eqs 14 and 15, Supporting Information).[64−66]

The Cr 2p spectra in Figure 6f show that the 2p3/2 line is centered at 577.6 eV, and the spin orbit splitting is 9.9 ± 0.1 eV, which is characteristic of Cr(III). The binding energy lying between 579 and 579.8 eV is the 2p3/2 of Cr(VI).[67] The increase in chromium atomic percent with pH dropping indicates enhanced Cr(VI) removal onto the composite in acidic solutions. Most chromium exists in trivalent form on the surface as a result of the dominated Cr(VI) reduction and the subsequent adsorption, and some is present as hexavalent chromium on account of the electrostatic attraction between the positively charged surface and Cr(VI) anions. According to Mullet's report,[22,67] Cr(III) could also exist as a mixed Fe(III)−Cr(III) solid on the FeS/Fe surface at pH greater than 4 (eq 16, Supporting Information).

As is known, Cr(VI) removal from aqueous phase by pure activated carbon usually depends on the surface adsorption and reducing action of surface organic groups.[45] On that basis, the reducibility of FeS/Fe will further enhance it. Therefore, Cr(VI) removal by the C/FeS/Fe composite mainly includes the following aspects: (a) adsorption of chromium by van der Waals force, (b) electrostatic attraction to Cr(VI) anions by the protonated carbon surface in acidic medium, (c) reduction of Cr(VI) by electron-donating groups and release of Cr(III), (d) positively charged Cr(III) binding to functional groups (−COO−, $-SO_3-$) through competition with H^+, (e) reduction of Cr(VI) by FeS/Fe and similar Cr(III) immobilization as (d), and (f) Cr(III) immobilization on the FeS/Fe surface in the form of a Fe(III)−Cr(III) solid at pH > 4.

Because the pH value is an important external factor, the effects of initial pH on Cr(VI) removal kinetics and Cr concentration are investigated. The removal efficiency of Cr(VI) increases from 31.7% to over 98% as pH deceases from 10 to 2 (Figure 7a), and the initial removal amount for 30 min accounts for more than 80% of its equilibrium value at pH > 4; however, this percentage decreases to 60% at pH 2, indicating more Cr(VI) will be removed in the subsequent hours in a strong acid environment. The reason may be that Cr(VI) removal primarily relies on the carbon surface at pH > 4 when FeS/Fe reduction of Cr(VI) is limited by the Fe(III)−Cr(III) solid layer,[22] but as pH gets lower, the strong acidic solution can gradually soak into the inner part of carbon, dissolving the embedded FeS/Fe over time and producing more reducing ions to work. The removal kinetics under different pH are investigated by two commonly used models, namely, pseudo-first-order and pseudo-second-order models (Figure S3, Supporting Information).[57,68] The pseudo-second-order model fits the experimental data quite well with all correlation coefficients near 0.99, and the pseudo-second-order rate constant increases from 0.000163 to 0.0014 g/mg/min with pH increasing from 2 to 10 (Table S3, Supporting Information), further indicating that low pH is favorable for Cr(VI) removal.

The concentration of Cr species and iron release at different pH are shown in Figure 7b. The Cr(VI) concentration is near 0 mg/L at pH 2 with more than 98% being removed and continuously increases with pH increasing. Unfortunately, the low pH value will bring about too much iron leakage into water. The minimum concentration of total Cr appears at pH 4 with 60% removed from the solution, suggesting that pH 4 is the best value in view of the removal of total Cr by C/FeS/Fe composite. The Cr(III) concentration reveals a contrary tendency to Cr(VI) because the reduction of solution acidity will be against the conversion of Cr(VI) into Cr(III), reducing the competition of protons with Cr(III) and being beneficial to Cr(III) immobilization on carbon. The minimum concentration of Cr(III) appears at pH 5. The results suggest that a pH value around 4 should be chosen in practical usage in comprehensive consideration of the removal of Cr(VI) and total Cr as well as the leakage of iron, although pH 2 is the best for Cr(VI) removal by the C/FeS/Fe composite.

Sorption isotherm experiments have been conducted at pH 5 with 10 various initial concentrations of Cr(VI) from 10 to 100 mg/L. Two common models of Langmuir and Freundlich isotherms[12,57] are used to fit the equilibrium data to determine the isotherm constants (Figure S4, Supporting Information). The as-fitted parameters (Table S4, Supporting Information) show that the equilibrium concentration and Cr(VI) removal amount increase with the initial concentrations, and both the Langmuir and Freundlich models with the R^2 values higher than 0.97 correlate the sorption isotherms well, implying that both chemisorption and physisorption exist in the adsorption systems.[46] The maximum Cr(VI) removal calculated from the Langmuir isotherm is 127 mg/g, which is much higher than those of some reported materials[69−73] such as iron-containing bamboo charcoal and nanosized magnetite-coated activated carbon (Table S5, Supporting Information). The results indicate that the C/FeS/Fe composite is a potential material for removing Cr(VI) from polluted water.

■ ASSOCIATED CONTENT

Supporting Information

Chemical equations, pore size distributions, XRD patterns after Cr(VI) removal, surface elemental composition, kinetic models and their fitted curves and parameters, and Langmuir and Freundlich models and their fitted curves and parameters. This material is available free of charge via the Internet at http://pubs.acs.org.

■ AUTHOR INFORMATION

Corresponding Author

*Tel.: 86-10-64436736. Fax: 86-10-64436736. E-mail: yangru@bbn.cn.

Notes

The authors declare no competing financial interest.

■ ACKNOWLEDGMENTS

We greatly acknowledge the financial support by the National Natural Science Foundation of China (51372012).

■ REFERENCES

(1) Dias, J. M.; Alvim-Ferraz, M. C. M.; Almeida, M. F.; Rivera-Utrilla, J.; Sánchez-Polo, M. Waste materials for activated carbon preparation and its use in aqueous-phase treatment: A review. *J. Environ. Manage.* **2007**, *85*, 833−846.

(2) De Ridder, D. J.; Villacorte, L.; Verliefde, A. R. D.; Verberk, J. Q. J. C.; Heijman, S. G. J.; Amy, G. L.; Van Dijk, J. C. Modeling equilibrium adsorption of organic micropollutants onto activated carbon. *Water Res.* **2010**, *44*, 3077−3086.

(3) Ramesha, G. K.; Vijaya Kumara, A.; Muralidhara, H. B.; Sampath, S. Graphene and graphene oxide as effective adsorbents toward anionic and cationic dyes. *J. Colloid Interface Sci.* **2011**, *361*, 270−277.

(4) Liang, C.; Lee, P. H. Granular activated carbon/pyrite composites for environmental application: Synthesis and characterization. *J. Hazard. Mater.* **2012**, *231−232*, 120−126.

(5) Gollavelli, G.; Chang, C. C.; Ling, Y. C. Facile synthesis of smart magnetic graphene for safe drinking water: heavy metal removal and disinfection control. *ACS Sustainable Chem. Eng.* **2013**, *1*, 462−472.

(6) Gheju, M.; Balcu, I. Removal of chromium from Cr(VI) polluted wastewaters by reduction with scrap iron and subsequent precipitation of resulted cations. *J. Hazard. Mater.* **2011**, *196*, 131−138.

(7) Current Drinking Water Regulations. Ground Water and Drinking Water, U.S. Environmental Protection Agency. http://water.epa.gov/lawsregs/rulesregs/sdwa/currentregulations.cfm.

(8) Chromium Slays Pollution Control and Environmental Protection. Technical Specifications. State Ministry of Environmental Protection (MEP): 2007.

(9) Cieslak-Golonka, M. Toxic and mutagenic effects of chromium-(VI): A review. *Polyhedron* **1995**, *15*, 3667−3689.

(10) Kotas, J.; Stasicka, Z. Chromium occurrence in the environment and methods of its speciation. *Environ. Pollut.* **2000**, *107*, 263−283.

(11) Fang, J.; Gu, Z.; Gang, D.; Liu, C.; Ilton, E. S.; Deng, B. Cr (VI) removal from aqueous solution by activated carbon coated with quaternized poly (4-vinylpyridine). *Environ. Sci. Technol.* **2007**, *41*, 4748−4753.

(12) Ghosh, P. K. Hexavalent chromium [Cr(VI)] removal by acid modified waste activated carbons. *J. Hazard. Mater.* **2009**, *171*, 116−122.

(13) Shevchenko, N.; Zaitsev, V.; Walcarius, A. Bifunctionalized mesoporous silicas for Cr(VI) reduction and concomitant Cr(III) immobilization. *Environ. Sci. Technol.* **2008**, *42*, 6922−6928.

(14) Guo, J.; Li, Y.; Dai, R.; Lan, Y. Rapid reduction of Cr(VI) coupling with efficient removal of total chromium in the coexistence of Zn(0) and silica gel. *J. Hazard. Mater.* **2012**, *243*, 265−271.

(15) Zhang, Y. C.; Li, J.; Zhang, M.; Dionysiou, D. D. Size-tunable hydrothermal synthesis of SnS_2 nanocrystals with high performance in visible light-driven photocatalytic reduction of aqueous Cr(VI). *Environ. Sci. Technol.* **2011**, *45*, 9324−9331.

(16) Kassem, T. S. Kinetics and thermodynamic treatments of the reduction of hexavalent to trivalent chromium in presence of organic sulphide compounds. *Desalination* **2010**, *258*, 206−218.

(17) He, Z.; Cai, Q.; Wu, M.; Shi, Y.; Fang, H.; Li, L.; Chen, J.; Chen, J.; Song, S. Photocatalytic reduction of Cr(VI) in an aqueous suspension of surface-fluorinated anatase TiO_2 nanosheets with exposed {001} facets. *Ind. Eng. Chem. Res.* **2013**, *52*, 9556−9565.

(18) Saha, B.; Orvig, C. Biosorbents for hexavalent chromium elimination from industrial and municipal effluents. *Coordin. Chem. Rev.* **2010**, *254*, 2959−2972.

(19) Shen, Y. S.; Wang, S. L.; Tzou, Y. M.; Yan, Y. Y.; Kuan, W. H. Removal of hexavalent Cr by coconut coir and derived chars——The effect of surface functionality. *Bioresour. Technol.* **2012**, *104*, 165−172.

(20) Gheju, M.; Iovi, A. Kinetics of hexavalent chromium reduction by scrap iron. *J. Hazard. Mater.* **2006**, *135*, 66−73.

(21) Patterson, R. R.; Fendorf, S. Reduction of hexavalent chromium by amorphous iron sulfide. *Environ. Sci. Technol.* **1997**, *31*, 2039−2044.

(22) Mullet, M.; Boursiquot, S.; Ehrhardt, J. J. Removal of hexavalent chromium from solutions by mackinawite, tetragonal FeS. *Colloids Surf., A* **2004**, *244*, 77−85.

(23) Wu, L.; Liao, L.; Lv, G.; Qin, F.; He, Y.; Wang, X. Micro-electrolysis of Cr(VI) in the nanoscale zero-valent iron loaded activated carbon. *J. Hazard. Mater.* **2013**, *254−255*, 277−283.

(24) Nethaji, S.; Sivasamy, A.; Mandal, A. B. Preparation and characterization of corn cob activated carbon coated with nano-sized magnetite particles for the removal of Cr(VI). *Bioresour. Technol.* **2013**, *134*, 94−100.

(25) Tang, L.; Yang, G. D.; Zeng, G. M.; Cai, Y.; Li, S. S.; Zhou, Y. Y.; Pang, Ya; Liu, Y. Y.; Zhang, Yi; Luna, B. Synergistic effect of iron doped ordered mesoporous carbon on adsorption-coupled reduction of hexavalent chromium and the relative mechanism study. *Chem. Eng. J.* **2014**, *239*, 114−122.

(26) Demoisson, F.; Mullet, M.; Humbert, B. Pyrite oxidation by hexavalent chromium: investigation of the chemical processes by monitoring of aqueous metal species. *Environ. Sci. Technol.* **2005**, *39*, 8747−8752.

(27) Bi, Y.; Yuan, Y.; Exstrom, C. L.; Darveau, S. A.; Huang, J. Air stable, photosensitive, phase pure iron pyrite nanocrystal thin films for photovoltaic application. *Nano Lett.* **2011**, *11*, 4953−4957.

(28) Li, W.; Döblinger, M.; Vaneski, A.; Rogach, A. L.; Jäckel, F.; Feldmann, J. Pyrite nanocrystals: shape-controlled synthesis and tunable optical properties via reversible self-assembly. *J. Mater. Chem.* **2011**, *21*, 17946−17952.

(29) Kadirvelu, K.; Kavipriya, M.; Karthika, C.; Radhika, M.; Vennilamani, N.; Pattabhi, S. Utilization of various agricultural wastes

for activated carbon preparation and application for the removal of dyes and metal ions from aqueous solutions. *Bioresour. Technol.* **2003**, *87*, 129−132.
(30) Li, W.; Yue, Q.; Tu, P.; Ma, Z.; Gao, B.; Li, J.; Xu, X. Adsorption characteristics of dyes in columns of activated carbon prepared from paper mill sewage sludge. *Chem. Eng. J.* **2011**, *178*, 197−203.
(31) Zhao, P.; Ge, S.; Ma, D.; Areeprasert, C.; Yoshikawa, K. Effect of hydrothermal pretreatment on convective drying characteristics of paper sludge. *ACS Sustainable Chem. Eng.* **2014**, *2*, 665−671.
(32) Li, Y.; Yue, Q.; Li, W.; Gao, B.; Li, J.; Du, J. Properties improvement of paper mill sludge-based granular activated carbon fillers for fluidized-bed bioreactor by bentonite (Na) added and acid washing. *J. Hazard. Mater.* **2011**, *197*, 33−39.
(33) Foo, K. Y.; Hameed, B. H. Mesoporous activated carbon from wood sawdust by K_2CO_3 activation using microwave heating. *Bioresour. Technol.* **2012**, *111*, 425−432.
(34) Wang, H.; Li, Z.; Tak, J. K.; Holt, C. M. B.; Tan, X.; Xu, Z.; Amirkhiz, B. S.; Harfield, D.; Anyia, A.; Stephenson, T.; Mitlin, D. Supercapacitors based on carbons with tuned porosity derived from paper pulp mill sludge biowaste. *Carbon* **2013**, *57*, 317−328.
(35) Liu, W.; Zhang, J.; Zhang, C.; Wang, Y.; Li, Y. Adsorptive removal of Cr(VI) by Fe-modified activated carbon prepared from *Trapa natans* husk. *Chem. Eng. J.* **2010**, *162*, 677−684.
(36) Yang, R.; Liu, G.; Li, M.; Zhang, J.; Hao, X. Preparation and N_2, CO_2 and H_2 adsorption of super activated carbon derived from biomass source hemp (*Cannabis sativa* L.) stem. *Microporous Mesoporous Mater.* **2012**, *158*, 108−116.
(37) Rosas, J. M.; Bedia, J.; Rodríguez-Mirasol, J.; Cordero, T. HEMP-derived activated carbon fibers by chemical activation with phosphoric acid. *Fuel* **2009**, *88*, 19−26.
(38) Yang, R.; Liu, G.; Xu, X.; Li, M.; Zhang, J.; Hao, X. Surface texture, chemistry and adsorption properties of acid blue 9 of hemp (*Cannabis sativa* L.) bast-based activated carbon fibers prepared by phosphoric acid activation. *Biomass Bioenergy* **2011**, *35*, 437−445.
(39) Wang, H.; Xu, Z.; Kohandehghan, A.; Li, Z.; Cui, K.; Tan, X.; Stephenson, T. J.; King'ondu, C. K.; Holt, C. M. B.; Olsen, B. C.; Tak, J. K.; Harfield, D.; Anyia, A. O.; Mitlin, D. Interconnected carbon nanosheets derived from hemp for ultrafast supercapacitors with high energy. *ACS Nano* **2013**, *7*, 5131−5141.
(40) Rosas, J. M.; Bedia, J.; Rodríguez-Mirasol, J.; Cordero, T. Preparation of hemp-derived activated carbon monoliths. Adsorption of water vapor. *Ind. Eng. Chem. Res.* **2008**, *47*, 1288−1296.
(41) Altundogan, H. S. Cr(VI) removal from aqueous solution by iron(III) hydroxide-loaded sugar beet pulp. *Process Biochem.* **2005**, *40*, 1443−1452.
(42) Huuska, M.; Koskenlinna, M.; Niinistö, L. Thermal decomposition of iron sulphates II. Mechanism of isothermal decomposition of $FeSO_4 \cdot H_2O$ in carbon monoxide. *Thermochim. Acta* **1975**, *13*, 315−320.
(43) Dufour, A.; Girods, P.; Masson, E.; Rogaume, Y.; Zoulalian, A. Synthesis gas production by biomass pyrolysis: Effect of reactor temperature on product distribution. *Int. J. Hydrogen Energy* **2009**, *34*, 1726−1734.
(44) Wang, C.; Chen, J. J.; Shi, Y. N.; Zheng, M. S.; Dong, Q. F. Preparation and performance of a core-shell carbon/sulfur material for lithium/sulfur battery. *Electrochim. Acta* **2010**, *55*, 7010−7015.
(45) Liu, S.; Sun, J.; Huang, Z. Carbon spheres/activated carbon composite materials with high Cr(VI) adsorption capacity prepared by a hydrothermal method. *J. Hazard. Mater.* **2010**, *173*, 377−383.
(46) Liu, W.; Zhang, J.; Zhang, C.; Ren, L. Preparation and evaluation of activated carbon-based iron-containing adsorbents for enhanced Cr(VI) removal: Mechanism study. *Chem. Eng. J.* **2012**, *189−190*, 295−302.
(47) Selvaraj, M.; Sinha, P. K.; Pandurangan, A. Synthesis of dypnone using SO_4^{2-}/Al-MCM-41 mesoporous molecular sieves. *Microporous Mesoporous Mater.* **2004**, *70*, 81−91.
(48) Socrates, G. *Infrared and Raman Characteristic Group Frequencies*; Wiley: New York, 2005.
(49) Shevchenko, N.; Zaitsev, V. Bifunctionalized mesoporous silicas for Cr(VI) reduction and concomitant Cr(III) immobilization. *Environ. Sci. Technol.* **2008**, *42*, 6922−6928.
(50) Zaitseva, N.; Zaitsev, V.; Walcarius, A. Chromium(VI) removal via reduction-sorption on bi-functional silica adsorbents. *J. Hazard. Mater.* **2013**, *250−251*, 454−461.
(51) Sing, K. S. W.; Everett, D. H.; Haul, R. A. W.; Moscou, L.; Pierotti, R. A.; Rouquérol, J.; Siemieniewska, T. Reporting physisorption data for gas/solid systems. *Pure Appl. Chem.* **1985**, *57*, 603−619.
(52) Lorenc-Grabowska, E.; Gryglewicz, G.; Gryglewicz, S. Development of mesoporosity in activated carbons via coal modification using Ca- and Fe-exchange. *Microporous Mesoporous Mater.* **2004**, *76*, 193−201.
(53) Yue, Z.; Bender, S. E.; Wang, J.; Economy, J. Removal of chromium Cr(VI) by low-cost chemically activated carbon materials from water. *J. Hazard. Mater.* **2009**, *166*, 74−78.
(54) Ma, H. L.; Zhang, Y.; Hu, Q. H.; Yan, D.; Yu, Z. Z.; Zhai, M. Chemical reduction and removal of Cr (VI) from acidic aqueous solution by ethylenediamine-reduced graphene oxide. *J. Mater. Chem.* **2012**, *22*, 5914−5916.
(55) Wei, S.; Li, D.; Huang, Z.; Huang, Y.; Wang, F. High-capacity adsorption of Cr(VI) from aqueous solution using a hierarchical porous carbon obtained from pig bone. *Bioresour. Technol.* **2013**, *134*, 407−411.
(56) Zhou, J. H.; Sui, Z. J.; Zhu, J.; Li, P.; Chen, D.; Dai, Y. C.; Yuan, W. K. Characterization of surface oxygen complexes on carbon nanofibers by TPD, XPS and FT-IR. *Carbon* **2007**, *45*, 785−796.
(57) Yuan, P.; Fan, M.; Yang, D.; He, H.; Liu, D.; Yuan, A.; Zhu, J.; Chen, T. Montmorillonite-supported magnetite nanoparticles for the removal of hexavalent chromium from aqueous solutions. *J. Hazard. Mater.* **2009**, *166*, 821−829.
(58) Abdel-Samad, H.; Watson, P. R. An XPS study of the adsorption of chromate on goethite (α-FeOOH). *Appl. Surf. Sci.* **1997**, *108*, 371−377.
(59) Siriwardane, R. V.; Poston, J. A., Jr.; Fisher, E. P.; Shen, M. S.; Miltz, A. L. Decomposition of the sulfates of copper, iron (II), iron (III), nickel, and zinc: XPS, SEM, DRIFTS, XRD, and TGA study. *Appl. Surf. Sci.* **1999**, *152*, 219−236.
(60) Fontecha-Cámara, M. A.; Álvarez-Merino, M. A.; Carrasco-Marín, F.; López-Ramón, M. V.; Moreno-Castilla, C. Heterogeneous and homogeneous Fenton processes using activated carbon for the removal of the herbicide amitrole from water. *Appl. Catal., B* **2011**, *101*, 425−430.
(61) Qiu, S. R.; Lai, H. F.; Roberson, M. J.; Hunt, M. L.; Amrhein, C.; Giancarlo, L. C.; Flynn, G. W.; Yarmoff, J. A. Removal of contaminants from aqueous solution by reaction with iron surfaces. *Langmuir* **2000**, *16*, 2230−2236.
(62) Liu, F.; Sun, J.; Sun, Q.; Zhu, L.; Wang, L.; Meng, X.; Qi, C.; Xiao, F. S. High-temperature synthesis of magnetically active and SO_3H-functionalized ordered mesoporous carbon with good catalytic performance. *Catal. Today* **2012**, *186*, 115−120.
(63) choi, Y.; Kim, Y.; Kang, K. Y.; Lee, J. S. A composite electrolyte membrane containing high-content sulfonated carbon spheres for proton exchange membrane fuel cells. *Carbon* **2011**, *49*, 1367−1373.
(64) Kim, C.; Zhou, Q. H.; Deng, B. L.; Thornton, E. C.; Xu, H. F. Chromium(VI) reduction by hydrogen sulfide in aqueous media: stoichiometry and kinetics. *Environ. Sci. Technol.* **2001**, *35*, 2219−2225.
(65) Lan, Y.; Kim, C.; Deng, B. L.; Thornton, E. C.; Xu, H. F. Catalysis of elemental sulfur nanoparticles on chromium(VI) reduction by sulfide under anaerobic conditions. *Environ. Sci. Technol.* **2005**, *39*, 2087−2094.
(66) Velasco, A.; Ramírez, M.; Hernández, S.; Schmidt, W.; Revah, S. Pilot scale treatment of chromite ore processing residue using sodium sulfide in single reduction and coupled reduction/stabilization processes. *J. Hazard. Mater.* **2012**, *207−208*, 97−102.
(67) Boursiquot, S.; Mullet, M.; Ehrhardt, J. J. XPS study of the reaction of chromium(VI) with mackinawite (FeS). *Surf. Interface Anal.* **2002**, *34*, 293−297.

(68) Kobya, M. Removal of Cr(VI) from aqueous solutions by adsorption onto hazelnut shell activated carbon: kinetic and equilibrium studies. *Bioresour. Technol.* **2004**, *91*, 317−321.
(69) Prabhakaran, S. K.; Vijayaraghavan, K.; Balasubramanian, R. Removal of Cr (VI) ions by spent tea and coffee dusts: reduction to Cr (III) and biosorption. *Ind. Eng. Chem. Res.* **2009**, *48*, 2113−2117.
(70) Wang, X. J.; Wang, Y.; Wang, X.; Liu, M.; Xia, S. Q.; Yin, D. Q.; Zhang, Y. L.; Zhao, J. F. Microwave-assisted preparation of bamboo charcoal-based iron-containing adsorbents for Cr(VI) removal. *Chem. Eng. J.* **2011**, *174*, 326−332.
(71) Li, Y.; Zhu, S.; Liu, Q.; Chen, Z.; Gu, J.; Zhu, C.; Lu, T.; Zhang, D.; Ma, J. N-doped porous carbon with magnetic particles formed in situ for enhanced Cr (VI) removal. *Water Res.* **2013**, *47*, 4188−4197.
(72) Wang, Y.; Wang, X. J.; Liu, M.; Wang, X.; Wu, Z.; Yang, L. Z.; Xia, S. Q.; Zhao, J. F. Cr(VI) removal from water using cobalt-coated bamboo charcoal prepared with microwave heating. *Ind. Crop. Prod.* **2012**, *39*, 81−88.
(73) Yuan, P.; Liu, D.; Fan, M.; Yang, D.; Zhu, R.; Ge, F.; Zhu, J. X.; He, H. Removal of hexavalent chromium [Cr(VI)] from aqueous solutions by the diatomite-supported/unsupported magnetite nanoparticles. *J. Hazard. Mater.* **2010**, *173*, 614−621.